Journal of
Mechanics of
Materials and Structures

WRINKLED MEMBRANES
PART II: ANALYTICAL MODELS

Y. Wesley Wong and Sergio Pellegrino

Volume 1, Nº 1 January 2006

mathematical sciences publishers

JOURNAL OF MECHANICS OF MATERIALS AND STRUCTURES
Vol. 1, No. 1, 2006

WRINKLED MEMBRANES PART II: ANALYTICAL MODELS

Y. WESLEY WONG AND SERGIO PELLEGRINO

We present a general analytical model for determining the location and pattern of wrinkles in thin membranes and for making preliminary estimates of their wavelength and amplitude. A rectangular membrane under simple shear and a square membrane subject to corner loads are analysed. In the first problem, our model predicts the wavelength and the wrinkle amplitude to be respectively inversely proportional and directly proportional to the fourth root of the shear angle. Both values are directly proportional to the square root of the height and thickness of the membrane, and are independent of the Young's modulus. In the second problem two wrinkling regimes are identified. The first regime is characterised by radial corner wrinkles and occurs for load ratios less than $1/(\sqrt{2}-1)$; the number of wrinkles is proportional to the fourth root of the radius of the wrinkled region and the magnitude of the corner force, and inversely proportional to the Young's modulus and thickness cubed. The amplitude of these wrinkles is inversely proportional to their number, directly proportional to the square root of the radius of the wrinkled region and the magnitude of the corner force, and inversely proportional to the square root of the Young's modulus and thickness. The second regime occurs for load ratios larger than $1/(\sqrt{2}-1)$, and is characterised by a large diagonal wrinkle, plus small radial wrinkles at all four corners. Analytical expressions for the variation of the width and amplitude of the large wrinkle with the load ratio are obtained for this case also. All analytical predictions are compared with experimental and computational results from the other two papers in this series.

1. Introduction

This is the second paper in a three-part series that deals with estimating wrinkle details, i.e. shape, wavelength, and amplitude, in thin, initially flat and stress-free membranes subject to certain prescribed in-plane load and boundary conditions.

The first paper [Wong and Pellegrino 2005a] presented an experimental study of two different problems. First, a rectangular membrane whose longer edges are sheared uniformly, and thus forms a "parallelogram" of approximately uniform wrinkles at 45° to the edges. Second, a square membrane loaded by two pairs

Keywords: complementary strain energy bounds, membrane structures, wrinkling.

of equal and opposite diagonal forces applied at the corners, which forms fans of uniform corner wrinkles if the ratio between the larger pair of forces and the smaller ones is less than about 2.5, but forms a large diagonal wrinkle aligned with the pair of larger forces if the ratio is higher than 2.5. A particularly interesting feature of the second problem is the change in the wrinkle pattern in response to changes in the force ratio. Detailed measurements of the shape of the wrinkles were made, and trends in the variation of the wavelength and amplitude were observed in each case.

The present paper presents a simple analytical model for heavily wrinkled membranes. This model is able to explain many features of the behaviour observed in the experiments and leads to a general method for making approximate estimates of both the overall wrinkle pattern and the average wrinkle amplitude and wavelength. This method is then applied to the sheared membrane and the square membrane problems, and analytical expressions are obtained in each case for the wrinkle wavelength and amplitude. Finally, the predictions made from these expressions are compared with the experimental results from [Wong and Pellegrino 2005a] and computational results from [Wong and Pellegrino 2005b], and are found to be remarkably accurate.

The layout of the paper is as follows. Section 2 presents a brief review of the literature on analytical methods for determining the extent of the wrinkle region and, within it, the direction of the wrinkles. Here the classical assumption is that the bending stiffness of the membrane is negligible, and hence an infinitely large number of vanishingly small wrinkles should form. A more detailed review of the recent literature; in which the bending stiffness of the membrane is no longer neglected, is then presented. Solutions for uniform, parallel wrinkle amplitudes have been published. Section 3 outlines the key ideas of our simple analytical model. Section 4 applies this model to the sheared membrane; here the wrinkles are known to be at 45° to the edges and so the implementation of our analytical model is rather straightforward. Section 5 implements the model for the square membrane. Here no analytical characterization of the wrinkle region exists, and so a range of simple, approximate equilibrium stress fields are proposed; a criterion for selecting the best approximation (which depends on the ratio of corner loads) is suggested. The derivation of the wrinkle wavelength and amplitude then follows along similar lines to Section 4. Section 6 compares the analytical predictions obtained in Sections 4 and 5 with results from the other two papers in this series. Section 7 concludes the paper.

2. Review of previous analytical models

Membrane wrinkling has attracted much interest in the past, starting from the observation that the web of a thin-walled beam can carry loads well above the initial buckling value, which prompted the development of tension field theory by Wagner [1929]. Simpler and yet more general formulations of this theory were proposed by Reissner [1938] and Mansfield [1968; 1970; 1989].

Reissner explained this theory by considering a thin strip under shear. He noted that up to a certain intensity of the shear load a uniform state of shear stress is induced in the sheet. If the load is increased beyond this intensity buckling occurs; however, if the distance of the longer edges of the sheet is kept constant, the shear load can be increased without failure to an intensity much greater than that at which buckling first took place. The out-of-plane deformation of the sheet after wrinkles are formed has been characterised in the first paper in the present series.

Reissner noted that once wrinkles are formed, the strip is mainly stressed in tension along the wrinkles, while the compressive stress perpendicular to the wrinkles — which is the cause for the wrinkles — is small compared with the tensile stress. At this point the fundamental assumption of tension field theory is that this compressive stress, and also the bending stresses induced by the out-of-plane deformation, are negligible in comparison with the tensile stress. Therefore, the theory searches for plane stress solutions such that one principal stress is positive and the other is zero. This is done by considering an elastic, anisotropic material (whose material directions depend on the stress field) with modulus of elasticity $E_\eta = 0$, where η is the principal stress direction transverse to the wrinkles. Reissner showed that the line $\eta =$ constant is straight, and went on to derive expressions for the rotationally symmetric stress field in a sheet forming a circular annulus whose edges are sheared.

A generalization of this theory was later proposed by Mansfield [1968; 1970], who introduced the concept of a tension ray, defined by the trajectories of tensile principal stress (the wrinkle directions), which again must be straight. He showed that, given a wrinkled membrane whose boundaries are in part free and in part subjected to given planar displacements, the direction of the tension rays is such that the (stretching) strain energy is *maximised*. This results in a powerful variational technique with which Mansfield determined the tension rays in, among others, semi-infinite and finite length rectangular strips clamped to rigid tie rods (Figure 1). A comprehensive presentation of this work can be found in [Mansfield 1989].

With the same fundamental assumptions of the tension field theory, but allowing for finite strains, an alternative approach [Pipkin 1986] is to construct a *relaxed strain energy* such that if at a point both principal stretches are less than 1 (i.e.

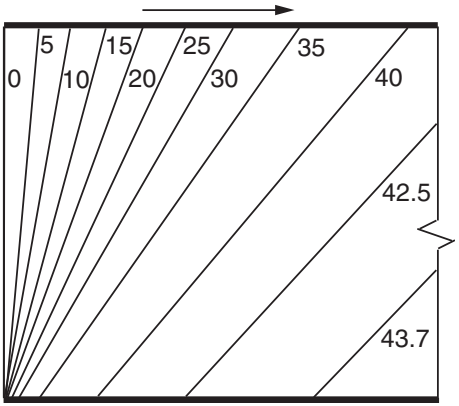

Figure 1. Tension rays in a semi-infinite membrane under simple shear, from [Mansfield 1989].

the membrane is slack) the relaxed strain energy is defined to be zero; if one principal stretch is greater than 1 the relaxed strain is defined on the basis of the larger stretch, and if both principal stretches are greater than 1 then a standard strain energy function is used. This formulation implicitly gets rid of compressive stresses, and has the advantage that it fits within a standard variational formulation. This approach was further developed and formalised by Steigmann [1990] and implemented numerically by Haseganu and Steigmann [1994] and Ligaro and Valvo [2000]. A generalization of the relaxed strain energy approach [Epstein and Forcinito 2001] in terms of a hyperelastic material which saturates when wrinkles form makes it easier to derive consistent expressions for the strain energy variations in the wrinkled state. Wu [1978], Wu and Canfield [1981], and Roddeman et al. [1987] have proposed to deal with wrinkling by modifying the deformation tensor such that the principal stress directions are either unchanged, in the case of isotropic membranes, or rotated appropriately in the case of anisotropic membranes.

Stein and Hedgepeth [1961] tackled the analysis of a partially wrinkled membrane, which can be divided into taut regions and wrinkled regions, by introducing the concept of a variable Poisson's ratio, which accounts for the geometric strains induced by wrinkling. These authors were able to obtain analytical solutions for, e.g., the moment-curvature relationship of a stretched rectangular membrane loaded by axial forces and bending moments at the ends. Here the wrinkles begin to form along the tension edge of the membrane, and propagate towards the neutral axis when the moment is increased.

A premise common to all of the above work is that a membrane is modelled as a *two-dimensional continuum unable to carry compression and with negligible*

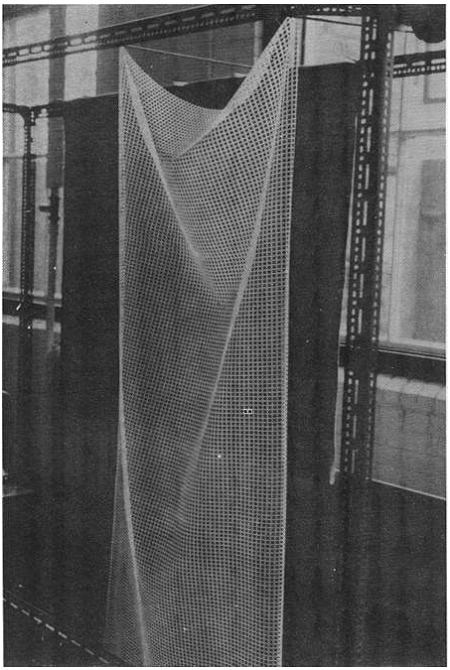

Figure 2. Wrinkles in a hanging "blanket", from [Rimrott and Cvercko 1986].

bending stiffness. Hence, it is implicitly assumed that an infinite number of wrinkles of infinitesimally small amplitude would form; it is generally believed that the stress fields produced by these theories are a good approximation to the stress fields in real membranes, when they are heavily wrinkled [Steigmann 1990]. Analytical solutions for the onset of wrinkles in rectangular membranes subject to uniaxial tension plus simple shear were obtained by Lin and Mote [1996]; these solutions incorporate, of course, the bending stiffness of the membrane.

The first study of the shape of a heavily wrinkled membrane (as opposed to the lightly corrugated shape that occurs soon after the onset of wrinkles) which also took into account the role played by the membrane bending stiffness was the "hanging blanket" solution by Rimrott and Cvercko [1986]. Consider a membrane held at two corner points at the same height. A number of curved wrinkles form under the action of gravity (Figure 2). The tension-line field, i.e., the stress distribution that occurs in the membrane if out-of-plane displacements are neglected and yet no compressive stress is allowed anywhere in the membrane, had previously been determined by Mansfield [1981] for the case of a rectangular blanket. Rimrott and Cvercko [1986] considered a membrane with sinusoidal, instead of straight boundaries, and for this particular case obtained a solution for the *post-wrinkling*

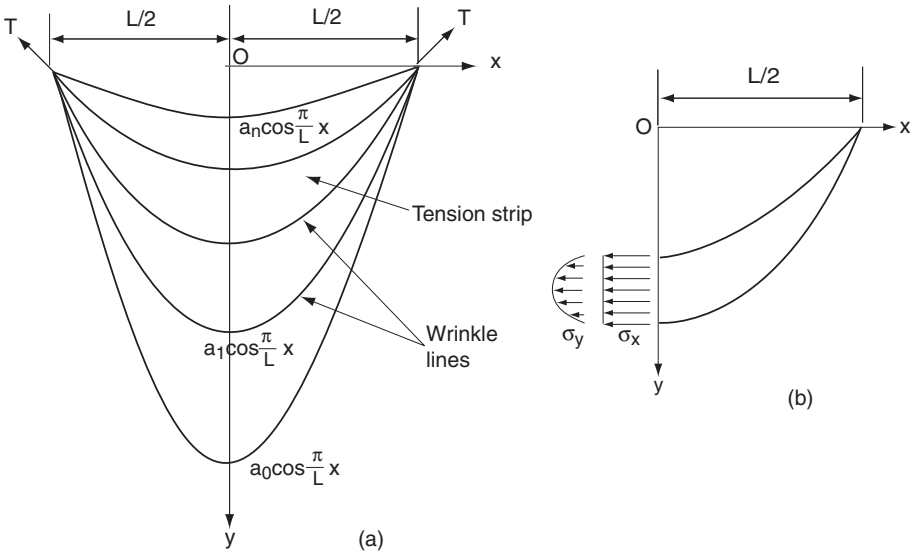

Figure 3. (a) Tension strips in hanging blanket and (b) detail of third tension strip, showing stress distribution along centre line, from Rimrott and Cvercko [1986].

tension-line field, where the membrane deforms out of plane while forming a number of wrinkles.

Rimrott and Cvercko noted that equilibrium of the membrane in the out-of-plane distorted configuration requires each finite-size wrinkle to carry a uniform horizontal force component; this horizontal force is equal in each wrinkle. Hence, having shown that the boundaries of the wrinkle lines (Figure 3) have amplitudes $a_n, \ldots, a_0$ that form a geometric progression ($a_i/a_{i+1} = \text{constant}$) it follows that the horizontal stress component, σ_x, at the centre of the wrinkle is largest in the more closely spaced wrinkles at the top of the membrane. Associated with σ_x, there is a compressive stress σ_y that vanishes at the edges of each finite-size wrinkle and reaches a maximum along the centre line of the wrinkle; see Figure 3(b). Rimrott and Cvercko assumed that the critical value, σ_{cr}, of this compressive stress is a characteristic of the blanket material and showed that for any chosen value of σ_{cr} there is corresponding number of finite-sized tension strips in the membrane.

Instead of Rimrott and Cvercko's "material constant", we have used for σ_{cr} the Euler buckling stress of an infinitely long, thin plate of thickness t, Young's modulus E, and Poisson's ratio ν [Wong and Pellegrino 2002]. Hence,

$$\sigma_{\text{cr}} = -\frac{\pi^2 E t^2}{12(1-\nu^2)\lambda^2}, \tag{1}$$

where the width of the plate, λ, matches the unknown half-wavelength of the wrinkle. We derived expressions for the wrinkle wavelength and amplitude in a long, rectangular membrane in simple shear. This approach, which forms the basis for the methodology presented in this paper, was extended in [Wong et al. 2003] to square membranes loaded by corner forces.

Epstein [2003] set up an approximate strain-energy analysis of a field of uniform, parallel wrinkles. Having assumed the wrinkles to be of sinusoidal shape longitudinally and to form circular arcs transversally (the same assumption had also been made by Murphey et al. [2002]), Epstein showed that, given a longitudinal strain ϵ_ξ and wrinkling strain (transverse) ϵ_η, the wrinkle amplitude is

$$A = \sqrt{2kL(\bar{\xi} - \bar{\xi}^2)}, \tag{2}$$

where $k = \sqrt{3\epsilon_\eta^2 t^2/2\epsilon_\xi(1-\nu^2)}$ and $\bar{\xi} = \xi/L$ is a nondimensional length variable along the wrinkle (where L is the length of the wrinkle).

For the case of a square membrane of side length H, we have $\epsilon_\xi = \gamma/2$ and $\epsilon_\eta = \gamma(\nu-1)/2$, and Epstein obtained

$$A = \sqrt{\sqrt{\frac{3\gamma}{4(1-\nu^2)}}(1-\nu)\frac{\sqrt{2}Ht}{2}}. \tag{3}$$

Energy-based derivations of the amplitude and wavelength of uniform, parallel wrinkles in a rectangular sheet under tension were obtained by Cerda and Mahadevan [2003].

The model presented in the next sections unifies our previous solutions [Wong and Pellegrino 2002; 2003] and can be used to tackle other nonparallel, nonuniform wrinkle fields.

3. Analytical model: general features

Our analytical approach is in four parts, as follows.

First, we propose a two-dimensional stress field that involves no compression anywhere in the membrane; the regions where the minor principal stress is zero are then assumed to be wrinkled and the wrinkles are assumed to be aligned with the major principal stress directions. Ideally, both equilibrium and compatibility should be satisfied everywhere by this stress field, but analytical solutions in closed form (obtained by tension field theory, for example) exist only for simple boundary conditions. However, we will show in Section 6 that a carefully chosen, simple stress field that satisfies only equilibrium can provide quick solutions that are useful for preliminary design. When several such stress fields have been identified, an estimate of the complementary strain energy associated with each field is used to select the most accurate one. More accurate stress fields, leading to better estimates

of the wrinkle details, can be obtained, of course, from a two-dimensional finite element stress analysis using membrane elements.

Second, we note that the bending stiffness of the membrane is finite, although small, and hence a compressive stress will exist in the direction perpendicular to the wrinkles. Because of its comparatively small magnitude, this stress was neglected in the first part of the analysis. We assume that this compressive stress varies only with the half-wavelength, λ, of the wrinkles and set it equal to the critical buckling stress of a thin plate in uniaxial compression. By Euler's formula applied to a plate of unit width [Calladine 1983], we have

$$\sigma_{\mathrm{cr}} = -\frac{\pi^2 E t^2}{12(1-\nu^2)\lambda^2} \tag{4}$$

Thus, the stress across the wrinkles is a known function of the wrinkle wavelength.

Third, in each wrinkled region we describe the out-of-plane displacement of the membrane, w, in terms of an unknown magnitude, A, and sinusoidal shape functions in a ξ, η coordinate system. The ξ and η-axes are aligned with the principal curvature directions, i.e. tangent and transverse to the wrinkles, respectively, and the half-wavelengths of these shape functions correspond to the length and width of the wrinkles. Thus, w automatically vanishes along the boundaries of the wrinkled zone.

The equation of equilibrium in the out-of-plane direction for a membrane that is not subject to any out-of-plane loading can be written in the form

$$\sigma_\xi \kappa_\xi + \sigma_\eta \kappa_\eta = 0 \tag{5}$$

(see [Calladine 1983]), where κ_ξ and κ_η are the principal curvatures, which can be obtained by differentiation of w. Since the stress distribution along the wrinkles is known, from the stress field determined during the first part of the analysis, in the transverse direction it can be assumed that

$$\sigma_\eta = \sigma_{\mathrm{cr}} \tag{6}$$

Enforcing Equation (5) at a single point, the midpoint of a wrinkle will be chosen, provides an equation from which λ can be determined.

Fourth, the wrinkle amplitudes are estimated by considering the total transverse strain ϵ_η as the sum of two components, a material strain (due to Poisson's ratio effects) and a wrinkling strain (due to in-plane geometric contraction associated with out-of-plane displacement). The sum of these two strains must match the boundary conditions imposed, e.g. by the wrinkle-free regions of the membrane.

Next, this general wrinkle model will be employed to predict the wrinkle details in two specific examples.

4. Analysis of membrane in shear

Consider a flat rectangular membrane of length L, height H, and thickness t, with clamped long edges and short free edges. The upper edge is translated by an amount δ in the direction of the edge itself, thus subjecting the membrane to a state of simple shear that causes the formation of a series of wrinkles, as seen in Figure 4. A full explanation of the resulting wrinkle pattern was presented in [Wong and Pellegrino 2005a], but here we will focus on the uniform wrinkles at 45° to the edges, in the central part of the membrane.

Consider one of these uniform wrinkles in the central, uniformly wrinkled part of the membrane, depicted in Figure 5.

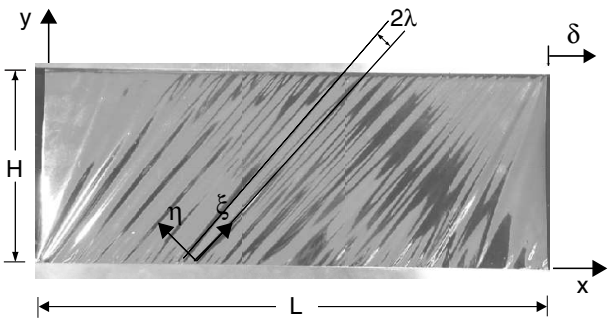

Figure 4. Rectangular Kapton sheet under simple shear.

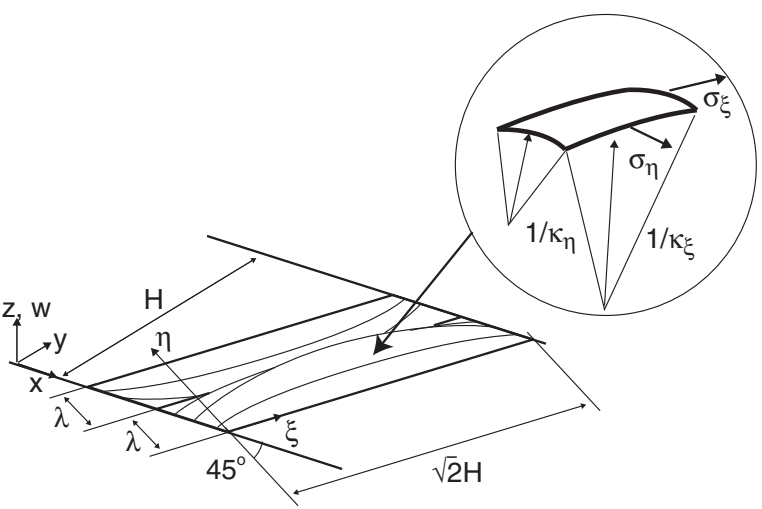

Figure 5. Perspective view of a single wrinkle.

Note that the initially flat membrane has deformed into a doubly-curved surface, alternately above and below the original xy plane of the membrane. This wrinkled surface intersects the xy plane at a regular spacing λ, defined as the half-wavelength of the wrinkle; neglecting edge effects, it can be assumed that these intersections occur along straight lines.

A simple mode-shape describing the wrinkled surface can be readily set up using the coordinate system ξ, η shown in Figure 5, where ξ is along the said intersection line, i.e. parallel to the wrinkle direction, and η is perpendicular to it. The boundary conditions on the out-of-plane displacement w are satisfied if we assume the mode shape

$$w = A \sin \frac{\pi(\xi + \eta)}{\sqrt{2}H} \sin \frac{\pi \eta}{\lambda} \tag{7}$$

Nothing is said at this stage about in-plane deflection. Since the wrinkles are long and narrow, $\eta \ll \xi$ apart from a small region near the origin. Hence, the mode shape can be simplified to

$$w \approx A \sin \frac{\pi \xi}{\sqrt{2}H} \sin \frac{\pi \eta}{\lambda} \tag{8}$$

The stress field consists of tension rays at 45° to the edges, and the stress along the wrinkles, σ_ξ, is much larger than the transverse stress, σ_η. Hence, neglecting σ_η when writing the stress-strain relationship in the ξ-direction, we obtain

$$\sigma_\xi = E \epsilon_\xi \tag{9}$$

For simple shear

$$\epsilon_\xi = \gamma/2 \tag{10}$$

where $\gamma = \delta/H$ and, substituting into Equation (9) we obtain

$$\sigma_\xi = E\gamma/2 \tag{11}$$

Recall that, although σ_η is relatively small in comparison with σ_ξ, in order for the wrinkle to have formed, the transverse stress must have reached the critical buckling stress given in (4).

The principal curvatures that appear in the equilibrium equation (5) can be determined as in [Calladine 1983] by differentiating (8):

$$\kappa_\xi = -\frac{\partial^2 w}{\partial \xi^2} = \frac{\pi^2 A}{2H^2} \sin \frac{\pi \xi}{\sqrt{2}H} \sin \frac{\pi \eta}{\lambda}, \tag{12}$$

$$\kappa_\eta = -\frac{\partial^2 w}{\partial \eta^2} = \frac{\pi^2 A}{\lambda^2} \sin \frac{\pi \xi}{\sqrt{2}H} \sin \frac{\pi \eta}{\lambda}. \tag{13}$$

These expressions are only exact where $\partial w/\partial \xi \approx 0$ and $\partial w/\partial \eta \approx 0$, which is indeed the case at a wrinkle mid point. Substituting Equations (4), (11), (12) and

(13) into (5), simplifying and rearranging yields for the wrinkle half-wavelength the expression

$$\lambda = \sqrt{\frac{\pi H t}{\sqrt{3(1-\nu^2)\gamma}}}. \tag{14}$$

To find an expression for the amplitude, A, of the wrinkle we note that the imposed strain ϵ_η, given by

$$\epsilon_\eta = -\gamma/2, \tag{15}$$

(as can be seen from Mohr's circle), has to be equal to the sum of the material strain

$$\epsilon_{\eta \mathrm{M}} = -\frac{\nu}{E}\sigma_\xi \tag{16}$$

with the average geometric strain, $\epsilon_{\eta \mathrm{G}}$, produced by wrinkling. This wrinkling strain is obtained by taking the difference between the projected width of a wrinkle and its actual width, and dividing by the actual width. Hence

$$\epsilon_{\eta \mathrm{G}} = \frac{\lambda - \displaystyle\int_0^\lambda \left(1 + \frac{1}{2}\left(\frac{\partial w}{\partial \eta}\right)^2\right) d\eta}{\displaystyle\int_0^\lambda \left(1 + \frac{1}{2}\left(\frac{\partial w}{\partial \eta}\right)^2\right) d\eta}. \tag{17}$$

Here, assuming the slope $\partial w/\partial \eta$ to be small, the term $(\partial w/\partial \xi)^2$ in the denominator can be neglected.

Next, consider the centre line across a wrinkle, and hence substitute $\xi = H/\sqrt{2}$ into (8). Substituting the resulting expression for w into (17) and working out the in integral gives

$$\epsilon_{\eta \mathrm{G}} = -\frac{\pi^2 A^2}{4\lambda^2}. \tag{18}$$

Finally, setting

$$\epsilon_\eta = \epsilon_{\eta \mathrm{M}} + \epsilon_{\eta \mathrm{G}} \tag{19}$$

as explained, we obtain

$$-\frac{\gamma}{2} = -\frac{\nu}{E}\sigma_\xi - \frac{\pi^2 A^2}{4\lambda^2}. \tag{20}$$

Substituting (11) into (20) and solving for A gives

$$A = \frac{\sqrt{2(1-\nu)\gamma}}{\pi}\lambda, \tag{21}$$

from which λ can be eliminated using Equation (14), to find

$$A = \sqrt{\frac{2Ht}{\pi}\sqrt{\frac{(1-\nu)\gamma}{3(1+\nu)}}}. \tag{22}$$

It can be readily verified that this expression is equivalent to that obtained by Epstein [2003], apart from a factor of 0.77. This discrepancy is mainly due to the fact that Epstein assumed circular arcs as the wrinkle mode shape, instead of a double sinusoid.

4.1. ***An energy approach.*** An alternative approach to find λ for the present, simple boundary conditions, is to set up an expression for the strain energy in a wrinkled thin plate, including the second-order strain due to out-of-plane deflection, and to minimize with respect to λ. The membrane is modelled as a thin plate stretched in the ξ-direction and wrinkled in the η-direction.

The general expression for the bending strain energy per unit area of an initially flat plate that is bent into a cylindrical shape of curvature κ_η is

$$U_b = \frac{1}{2}\frac{Et^3}{12(1-\nu^2)}\kappa_\eta^2. \tag{23}$$

As κ_η is not constant — see Equation (13) — the average strain energy per unit area, $\overline{U}_b$, is obtained from

$$\overline{U}_b = \frac{1}{2}\frac{Et^3}{12(1-\nu^2)}\left(\frac{1}{\sqrt{2}H\lambda}\int_0^{\lambda}\int_0^{\sqrt{2}H}\kappa_\eta^2\,d\xi\,d\eta\right) = \frac{1}{2}\frac{Et^3}{12(1-\nu^2)}\frac{\pi^4A^2}{4\lambda^4}. \tag{24}$$

The stretching strain energy per unit area can be obtained, neglecting stretching in the η-direction, from

$$U_s = \tfrac{1}{2}Et\epsilon_\xi^2. \tag{25}$$

Here, ϵ_ξ is the sum of the strain due to the in-plane shear, Equation (10), plus that due to the out-of-plane deflection due to wrinkling:

$$\epsilon_\xi = \frac{\gamma}{2} + \frac{1}{2}\left(\frac{\partial w}{\partial \xi}\right)^2. \tag{26}$$

Thus ϵ_ξ is also not constant. Hence, consider the average strain energy per unit area over a wrinkle, $\overline{U}_s$, given by

$$\overline{U}_s = \frac{1}{2}Et\left(\frac{1}{\sqrt{2}H\lambda}\int_0^{\lambda}\int_0^{\sqrt{2}H}\epsilon_\xi^2\,d\xi\,d\eta\right) \approx \frac{Et}{2}\frac{\gamma^2}{4} + \frac{Et}{2}\frac{\pi^2A^2\gamma}{16H^2}. \tag{27}$$

The first of these terms is independent of the wrinkle amplitude, A; therefore it will not be carried through to the next stage of the analysis.

The total mean strain energy per unit area (neglecting the term without A) is given by

$$\overline{U} = \overline{U}_b + \overline{U}_s = \frac{1}{2}\frac{Et^3}{12(1-\nu^2)}\frac{\pi^4A^2}{4\lambda^4} + \frac{Et}{2}\frac{\gamma^2}{4} + \frac{Et}{2}\frac{\pi^2A^2\gamma}{16H^2}. \tag{28}$$

Next, expressing A in terms of λ, Equation (21), we obtain

$$\overline{U} = \frac{(1-\nu)Et\gamma}{2}\left(\frac{\pi^2 t^2}{24(1-\nu^2)\lambda^2} + \frac{\gamma\lambda^2}{8H^2}\right). \tag{29}$$

Differentiating with respect to λ and setting $d\overline{U}/d\lambda = 0$ gives an expression equivalent to Equation (14). This result shows that the simple equilibrium formulation with an assumed stress σ_η, presented in Section 4, captures the same effects as the analytically more elaborate energy formulation.

5. Analysis of membrane under corner loads

The second problem considered in this paper is an initially flat, square membrane of side length $L+2a$ and thickness t, subjected to two pairs of equal and opposite corner forces, T_1 and T_2, as shown in Figure 6. Note that the actual corners of the membrane have been removed, and it is assumed that the concentrated loads are applied to the membrane through rigid beams of length d. We are interested in determining the wrinkle pattern for different values of the ratio T_1/T_2. This problem was investigated experimentally in [Wong and Pellegrino 2005a, Section 5].

A key difficulty in extending the approach of Section 3 to the present problem is that no tension field solution is known for this problem and so an approximate solution will be sought. We propose four different, no-compression "equilibrium" stress fields, some of which are only valid if the ratio of the corner forces is in a particular range. For each stress distribution an upper-bound estimate of the corner displacements will be obtained, and so, when for a given load ratio and membrane dimensions there is more than one potential stress distribution, the best

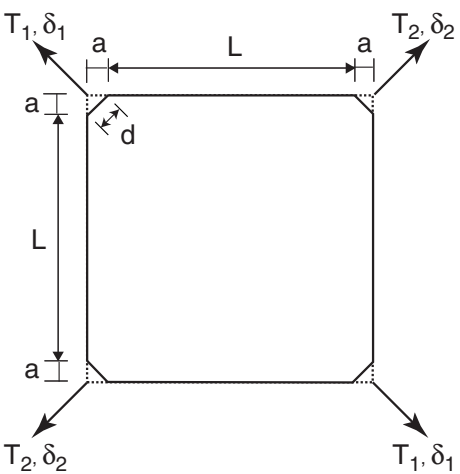

Figure 6. Square membrane subject to corner loads.

approximation to the actual stress field in the membrane will be obtained by choosing the particular distribution that produces the lowest upper bound for the corner deflections.

5.1. ***Stress fields.*** Figure 7 shows four possible stress fields, all of which satisfy equilibrium everywhere and involve no compressive stress at any point. In each case the membrane has been divided into regions that are either unloaded or subject to a simple state of stress. The stress field in Figure 7(b) is valid only for $T_1 = T_2$,

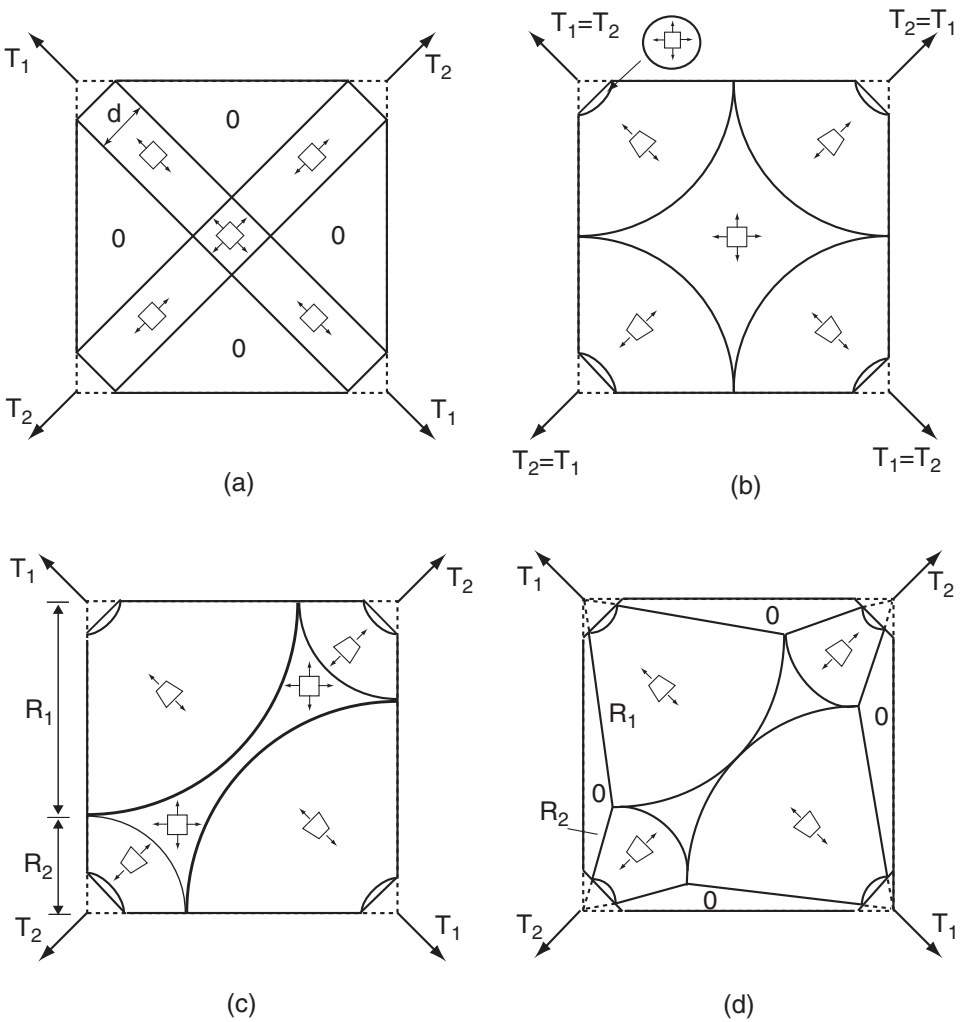

Figure 7. Equilibrium stress fields: (a) diagonal strip field; (b, c) wedge fields; (d) variable angle wedge field. A trapezium denotes a purely radial stress field.

while the others are more general, although still subject to some restrictions to be explained later.

Although equilibrium is satisfied, there is no guarantee that the elastic strains associated with these fields are compatible; indeed obvious compatibility violations can be easily detected for the simpler fields.

For each stress field it is possible to produce an estimate of the corresponding corner displacements, δ_1 and δ_2, defined in Figure 6. These displacements are computed using an upper-bound approach based on the complementary strain energy in the membrane.

The theorem of minimum complementary energy [Calladine 1983] states that the total complementary energy in a linear-elastic structure is minimum for the actual stress distribution. Hence, for an assumed stress field satisfying equilibrium but not necessarily compatibility, the complementary energy will be higher than for the actual stress distribution; thus

$$U \leqslant U^*, \tag{30}$$

where U and U^* are the actual and the estimated complementary energies. Hence, given a set of stress fields, we will define the "best" to be the stress field that produces the smallest estimate of U^*.

U^* can be calculated from

$$U^* = \frac{1}{2}\int_V (\epsilon_1\sigma_1 + \epsilon_2\sigma_2)\, dV, \tag{31}$$

where σ_i and ϵ_i denote the principal stresses and strains.

By conservation of energy, U is given for two given sets of corner forces, T_i, and corresponding corner displacements δ_i by

$$U = \frac{1}{2}\sum_{i=1}^{2} 2T_i\delta_i = T_1\delta_1 + T_2\delta_2. \tag{32}$$

Hence, from Equation (30), the average of the corner displacements, each weighted by the corresponding applied forces, determined by means of this method, is always an upper bound to the correct value.

Diagonal strip field. Figure 7(a) shows a simple stress field, consisting of four diagonal tension strips of width d, each under uniform uniaxial stress, plus a biaxially stressed centre region. The remaining parts of the membrane are unstressed.

For the case of symmetric loading, $T_1 = T_2 = T$ and $\delta_1 = \delta_2 = \delta$, the uniaxial stress in the tension strips is

$$\sigma_t = \frac{T}{dt} \tag{33}$$

and the complementary energy in each diagonal region is

$$U_1^* = \frac{1}{2}\int_V \frac{\sigma_t^2}{E} dV = \frac{T^2 L}{2\sqrt{2} d E t}, \tag{34}$$

whereas the complementary energy in the central biaxially stressed region is

$$U_2^* = \int_V \frac{\sigma_t^2 (1-\nu)}{E} dV = \frac{T^2 (1-\nu)}{E t}. \tag{35}$$

Hence, considering the four diagonal regions plus the central region, the total complementary energy for this stress field is

$$U^* = \frac{T^2}{E t}\left(\frac{\sqrt{2} L}{d} + (1-\nu)\right). \tag{36}$$

Therefore, the corner displacement, δ, can be determined from (30), (32), and (36) which give

$$\delta \leqslant \frac{T}{2 E t}\left(\frac{\sqrt{2} L}{d} + (1-\nu)\right). \tag{37}$$

Wedge field. The second stress field, shown in Figure 7(b), is for symmetric load cases, $T_1 = T_2 = T$ and $\delta_1 = \delta_2 = \delta$. This field is based around four identical wedges subject to purely radial stress, joined by a central region under uniform biaxial stress, and with small corner lunes also under uniform biaxial stress. Detailed views are shown in Figure 8.

The stress distribution in the wedge region, ABCD, is assumed to be purely radial and inversely proportional to the distance r from the apex O:

$$\sigma_r = \frac{T}{\sqrt{2} r t}, \tag{38}$$

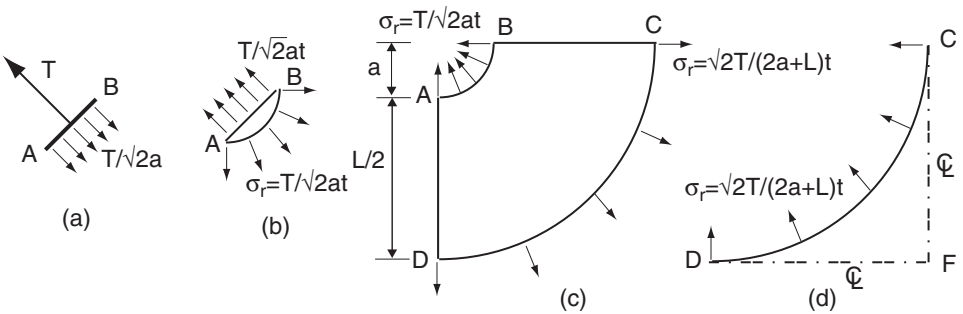

Figure 8. Components of wedge field: (a) free body diagram of edge beam; (b) biaxially stressed corner lune; (c) radially stressed wedge region; (d) one quarter of biaxially stressed centre region.

where $a < r < a + L/2$. Hence, the radial stress is uniform on any circular arc and all other stress components are zero. It can be readily shown that this distribution satisfies equilibrium, indeed this distribution was inspired from the classical plane-stress solution for a wedge-shaped thin plate [Timoshenko and Goodier 1970].

The radial stress along the curved edges of this wedge are equilibrated by two regions of uniform, biaxial stress: the lune AB and the central region defined by the arc CD and the symmetry lines CF and DF. The stress magnitudes in these two regions are obtained by substituting $r = a$ and $r = a + L/2$, respectively, into (38).

The complementary energy for each of these regions can be found by an approach analogous to that described in Section 5.1, although now the derivation is much lengthier as the integration of the complementary strain energy has to be carried out over several regions. Thus we obtain for the corner displacement the upper bound

$$\delta \leqslant \frac{T}{4Et}\left(\pi \ln\left(1 + \frac{L}{2a}\right) + 2(1-\nu)\right). \tag{39}$$

This type of stress field can be extended to asymmetric loading. Starting from the symmetric case described above, consider increasing T_1. For equilibrium to be still satisfied, the key requirement is that the radial stress along the four arcs bounding the central region should be uniform. Since now σ_r in each wedge region is proportional to T_i/r, we can compensate for the increase in T_1 by increasing correspondingly the outer radius of this wedge, or by decreasing the outer radius of the wedge corresponding to T_2, or both; see Figure 7(c). For the stress along the edges of the centre region to be uniform, clearly we require that $R_1/R_2 \propto T_1/T_2$.

This approach is valid until the two arcs of larger radius touch at the centre of the membrane, which happens when

$$\frac{R_1}{R_2} = \frac{T_1}{T_2} = \frac{1}{\sqrt{2}-1} \approx 2.41. \tag{40}$$

When $T_1 \neq T_2$ the corner displacements δ_1 and δ_2 are also different. Hence, computing the overall complementary energy does not lead to a bound on a particular corner displacement. A useful estimate of the radial corner displacements can be obtained by dividing the membrane into two parts, each associated with the displacements of a pair of opposite corners; the split is illustrated in Figure 9. For example, the corners loaded by T_1 are associated with the larger two wedges, plus the two areas labelled A_1.

The areas labelled A_1 and A_2 needed for the complementary strain energy calculation are given by

$$A_1 = \frac{(R_1+R_2)^2}{2} - \frac{\pi R_1^2}{4} - R_2^2 = \frac{1}{2}\left(1 - \frac{\pi}{2}\right) R_1^2 + R_1 R_2 - \frac{R_2^2}{2}$$

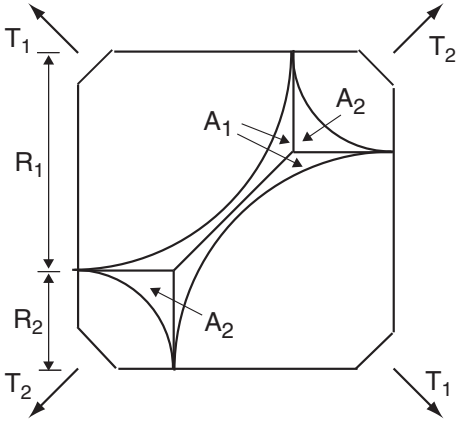

Figure 9. Partitioning of membrane for energy calculation.

and

$$A_2 = R_2^2 - \frac{\pi R_2^2}{4}.$$

Thus, after computing the complementary strain energy associated with each corner, we obtain

$$\delta_1 \leqslant \frac{T_1}{4Et}\left(\pi \ln \frac{R_1}{a} + \frac{1-\nu}{R_1^2}(4R_1R_2 - 2R_2^2)\right), \tag{41}$$

$$\delta_2 \leqslant \frac{T_2}{4Et}\left(\pi \ln \frac{R_2}{a} + 2(1-\nu)\right). \tag{42}$$

Note that, although Equations (41) and (42) are useful tools for design, they are not rigorous expressions, since their validity is not underpinned by the complementary energy theorem.

Variable angle wedge field. As stated earlier, the wedge stress field presented in Section 5.1 is only valid up to $T_1/T_2 \approx 2.41$. At this point the edges of the larger two wedges come into contact, thus forming a single region (continuous between the two most heavily loaded corners of the membrane) without tensile stress in the transverse direction. Note that the limit of 2.41 closely corresponds to the load ratio at which a diagonal wrinkle was first observed experimentally [Wong and Pellegrino 2005a].

A more general stress field, which allows us to consider larger values of T_1/T_2, has been shown in Figure 7(d). Here, the outer radius of the wedges corresponding to the larger loads is kept equal to the value at which the wedges meet at the centre of the membrane

$$R_1 = a + L/\sqrt{2} \tag{43}$$

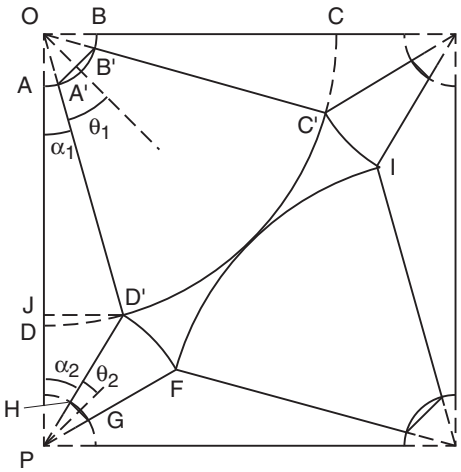

Figure 10. Geometry of variable angle wedge field.

but the angle subtended by these wedges, $2\theta_1$, is allowed to vary, depending on T_1/T_2. This has the effect that the outer radius of the remaining two wedges also varies.

Thus, this stress field consists of: four wedges subject to purely radial stress (A′B′C′D′, D′FGH, etc.); a central region under uniform biaxial stress (C′D′FI); and four corner lunes also under biaxial stress. This leaves four triangular edge regions that are unstressed. The acute angles of these triangles are related to the wedge half-angles by

$$\alpha_i = \frac{\pi}{4} - \theta_i. \tag{44}$$

The stress distribution in each of the four wedge regions is given by a generalization of (38) to a wedge subtending an angle of $2\theta_i$

$$\sigma_r = \frac{T_i}{2rt\sin\theta_i}. \tag{45}$$

Hence, the normal stress along the edges of C′D′FI is obtained by substituting $r = R_1$ and $r = R_2$ into (45), and for the two magnitudes to be equal we require

$$\frac{T_1}{2R_1 t\sin\theta_1} = \frac{T_2}{2R_2 t\sin\theta_2}. \tag{46}$$

Rearranging (46) we obtain the general condition

$$\frac{R_2\sin\theta_2}{\sin\theta_1} = \frac{R_1 T_2}{T_1}. \tag{47}$$

For any given T_1 and T_2, and since R_1 is known, R_2, θ_1, and θ_2 have to satisfy this condition.

Two additional conditions on R_2, θ_1, and θ_2 are obtained as follows. For the first condition, note that

$$\overline{JD'} = \overline{OD'}\sin\alpha_1 = R_1\sin\left(\frac{\pi}{4} - \theta_1\right) \tag{48}$$

and also

$$\overline{JD'} = \overline{PD'}\sin\alpha_2 = R_2\sin\left(\frac{\pi}{4} - \theta_2\right). \tag{49}$$

Equating these expressions for $\overline{JD'}$ and rearranging

$$R_2 = R_1\left(\sin\frac{\pi}{4} - \theta_1\right)\Big/\left(\sin\frac{\pi}{4} - \theta_2\right). \tag{50}$$

For the second condition, apply the sine rule to D′OP to obtain

$$\frac{R_1}{\sin\alpha_2} = \frac{2a + L}{\sin(\pi - \alpha_1 - \alpha_2)} \tag{51}$$

Substituting Equation (44) and grouping all unknowns on the right-hand side gives

$$\frac{\cos(\theta_1 + \theta_2)}{\sin\left(\frac{\pi}{4} - \theta_2\right)} = \frac{2a + L}{R_1}. \tag{52}$$

Equations (47), (50), and (52) can be solved for any given value of $T_1/T_2 > 1/(\sqrt{2} - 1)$ to determine the corresponding parameters of the stress field.

Figure 11 is a plot of the variation with T_1/T_2 of the angles that determine the four wedges, θ_1 and θ_2. Note that, since the wedge angles become smaller as T_1/T_2 increases, the slack regions along the edges of the membrane, denoted by a "0" in Figure 7(d), get bigger.

The complementary strain energy associated with each of the corner displacements is then calculated, splitting the central, biaxially stressed region into areas A_1 and A_2, which now have the expressions

$$A_1 = \frac{(2a + L)^2}{2} - R_1^2(\theta_1 + \sin\alpha_1\cos\alpha_1) - R_2^2\cos^2\alpha_2,$$
$$A_2 = R_2^2(\cos^2\alpha_2 - \theta_2 - \sin\alpha_2\cos\alpha_2).$$

Thus, following the same approach as in Section 5.1, we obtain

$$\delta_i \le \frac{T_i}{4Et\sin^2\theta_i}\left(2\theta_i\ln\frac{R_i}{a} + (1 - \nu)(\theta_i - \sin\theta_i\cos\theta_i) + \frac{A_i}{R_i^2}\right), \tag{53}$$

where i takes the values 1 or 2, depending on the corner of interest.

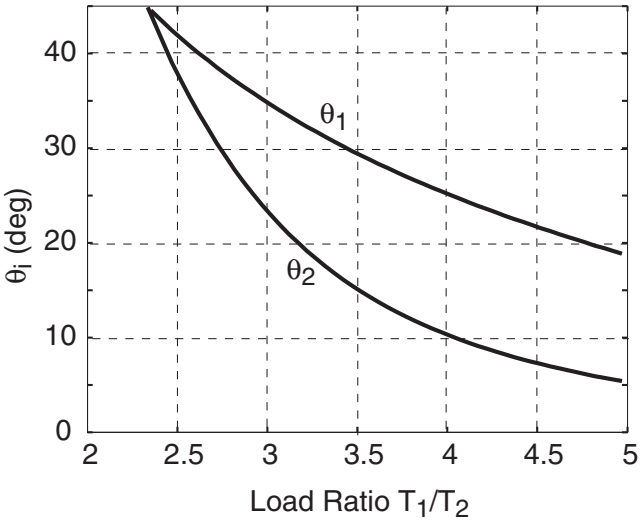

Figure 11. Geometric parameters of variable angle wedge field.

5.2. ***Wrinkle details.*** Based on the no-compression stress fields that have been proposed in Section 5.1, two different kinds of wrinkle patterns can be expected. Note that the diagonal strip stress field was included only for the sake of explanation but, as it does not lead to accurate estimates, it will not be used for any further analysis.

If $T_1/T_2 < 1/(\sqrt{2}-1)$, there is a biaxially stressed region at the centre of the membrane, separating four uniaxially stressed corner regions. Hence, four separate fans of wrinkles will form near the corners, but they cannot go through the centre. If $T_1/T_2 \geq 1/(\sqrt{2}-1)$, the two larger uniaxial stress regions join up at the centre of the membrane. Hence, there is a continuous, narrow diagonal region that is uniaxially stressed, and so in this case a small number of wrinkles can go all the way from one highly loaded corner to the other.

In the first case, we will assume each fan to consist of identical, radial wrinkles that start right at the edge of a biaxially stressed corner lune and extend as far as an unknown radius, R_w. This analysis can be more easily explained for the case of symmetric loading. In the second case, although fans of wrinkles will also form, we will focus on the much larger, diagonal wrinkle parallel to the loads T_1.

Corner wrinkles. Figure 12 shows a corner of a symmetrically loaded membrane. Here, R_{w} denotes the outer radius of the wrinkled zone, and it is assumed that the wrinkles start right at the edge of the biaxially stressed lune, AB. Note that in the region between R_w and R the formation of wrinkles is possible, because the stress is still uniaxial, but there isn't enough spare material for the wrinkles to actually

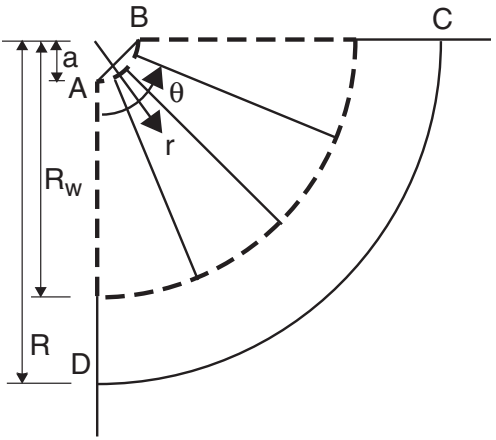

Figure 12. Region affected by fan of $n = 4$ half-wrinkles.

show. R denotes the outer radius of the wedge stress field, hence $R = a + L/2$ for symmetric loading. However, we will keep the more general notation.

The profile of the membrane in the wrinkled zone is assumed to be given by

$$w = A \sin \frac{\pi(r-a)}{R_w - a} \sin 2n\theta, \tag{54}$$

where the angle θ is measured from an edge of the membrane, A is an unknown amplitude, and n is the total number of half-wrinkles, each subtending an angle of $\pi/2n$. Note that the particular mode shape sketched in Figure 12 and assumed in Equation (54) sets the out-of-plane displacement of the membrane to zero along the edges, and assumes an integer number of half-wrinkles, for simplicity.

The value of n can be determined by considering out-of-plane equilibrium in the middle of a wrinkle. At such a point the principal directions of curvature are r and θ, and hence the equilibrium equation is

$$\sigma_r \kappa_r + \sigma_\theta \kappa_\theta = 0, \tag{55}$$

where κ_r and κ_θ are the radial and hoop curvatures obtained by differentiation of Equation (54). Hence,

$$\kappa_r = -\frac{\partial^2 w}{\partial r^2} = \frac{A\pi^2}{(R_w - a)^2} \sin \frac{\pi(r-a)}{R_w - a} \sin 2n\theta,$$

$$\kappa_\theta = -\frac{1}{r^2}\frac{\partial^2 w}{\partial \theta^2} = \frac{4An^2}{r^2} \sin \frac{\pi(r-a)}{R_w - a} \sin 2n\theta.$$

The centre of a wrinkle is the point where the curvatures are maximum, hence it is located at

$$\tilde{r} = \frac{R_w + a}{2} \tag{56}$$

The maximum curvatures are therefore

$$\tilde{\kappa_r} = \frac{A\pi^2}{(R_w - a)^2}, \qquad \tilde{\kappa_\theta} = \frac{16An^2}{(R_w + a)^2}. \tag{57}$$

The radial stress at the centre of the wrinkle is obtained by substituting Equation (56) into the general expression for the wedge field, Equation (38). Hence

$$\sigma_r = \frac{\sqrt{2}T}{(R_w + a)t}. \tag{58}$$

The hoop stress will be set equal to the critical buckling stress, Equation (4), with λ set equal to the central wrinkle half-wavelength, $\tilde{\lambda}$. Hence,

$$\tilde{\lambda} = \frac{\pi\tilde{r}}{2n} = \frac{\pi(R_w + a)}{4n}$$

and so

$$\sigma_\theta = -\frac{4Et^2n^2}{3(1-\nu^2)(R_w + a)^2}. \tag{59}$$

Substituting Equations (57), (58) and (59) into (55) and simplifying gives

$$\frac{\sqrt{2}\pi^2 T}{(R_w + a)(R_w - a)^2 t} - \frac{64Et^2n^4}{3(1-\nu^2)(R_w + a)^3} = 0,$$

from which, solving for n,

$$n = \sqrt[4]{\frac{3\sqrt{2}\pi^2(1-\nu^2)(R_w + a)^3}{64Et^3(R_w - a)^2}T}. \tag{60}$$

To find the amplitude, A, we equate the total hoop strain, obtained from the in-plane displacement field, to the sum of the material strain and the geometric strain due to the wrinkles.

The displacement field is assumed to be purely radial. Hence, denoting by $u(r)$ the radial displacement, defined to be positive in the positive r direction, we have

$$u = \int_R^r \epsilon_r dr = \int_R^r \frac{\sigma_r}{E} dr = \frac{T}{\sqrt{2}Et} \ln\frac{r}{R},$$

where it has been assumed that $u(R) \approx 0$. The hoop strain at the centre of a wrinkle is therefore

$$\tilde{\epsilon_\theta} = \frac{\tilde{u}}{\tilde{r}} = \frac{\sqrt{2}T}{Et(R_w + a)} \ln\frac{R_w + a}{2R}. \tag{61}$$

On the other hand, the material hoop strain and the geometric hoop strain due to the out-of-plane deformation associated with wrinkling, at the centre of a wrinkle, are respectively

$$\tilde{\epsilon}_{\theta\mathrm{M}} = -\nu\frac{\sigma_r}{E} = -\frac{\nu}{E}\frac{\sqrt{2}T}{(R_w+a)t}, \qquad \tilde{\epsilon}_{\theta\mathrm{G}} = -\frac{\pi^2 A^2}{4\tilde{\lambda}^2} = -\frac{4A^2n^2}{(R_w+a)^2}. \tag{62}$$

Hence, substituting Equations (61) and (62) into

$$\tilde{\epsilon}_\theta = \tilde{\epsilon}_{\theta\mathrm{M}} + \tilde{\epsilon}_{\theta\mathrm{G}}$$

and simplifying, we obtain

$$\frac{\sqrt{2}T}{Et}\ln\frac{R_w+a}{2R} = -\frac{\sqrt{2}\nu T}{Et} - \frac{4A^2n^2}{R_w+a}.$$

Solving for A we find

$$A = \frac{1}{n}\sqrt{\frac{R_w+a}{2\sqrt{2}Et}\left(\ln\frac{2R}{R_w+a} - \nu\right)T} \tag{63}$$

Finally, we can determine the value of the outer radius of the wrinkled region, R_w, by looking for the value of r at which the material hoop strain is the total hoop strain, and so $\epsilon_{\theta\mathrm{G}} = 0$. Hence, we substitute $r = R_w$ into general expressions for ϵ_θ and $\epsilon_{\theta\mathrm{M}}$, and then set $\epsilon_\theta = \epsilon_{\theta\mathrm{M}}$ to find

$$\frac{T}{\sqrt{2}EtR_w}\ln\frac{R_w}{R} = -\frac{\nu T}{\sqrt{2}EtR_w}, \tag{64}$$

from which, solving for R_w,

$$R_w = e^{-\nu}R. \tag{65}$$

Asymmetric loading. The analysis presented in the previous section can be generalised to cover the case of nonsymmetric loading with $1 < T_1/T_2 < 1/(\sqrt{2}-1)$, and can also be used to characterize the fans of corner wrinkles that occur when $T_1/T_2 > 1/(\sqrt{2}-1)$.

In the latter case, though, we are mainly interested in the largest wrinkle, which runs along the diagonal parallel to the loads T_1, as depicted in Figure 13. Incidentally, due to the narrowness of the region of contact between the two larger wedge stress fields, it is reasonable to assume that only a single large wrinkle will be able to form.

Consider the coordinate system ξ, η shown in the figure, with axes parallel and orthogonal to the wrinkle direction, and the simple mode shape

$$w = A\sin\frac{\pi\xi}{\sqrt{2}(L+a)}\sin\frac{\pi\eta}{\lambda} \tag{66}$$

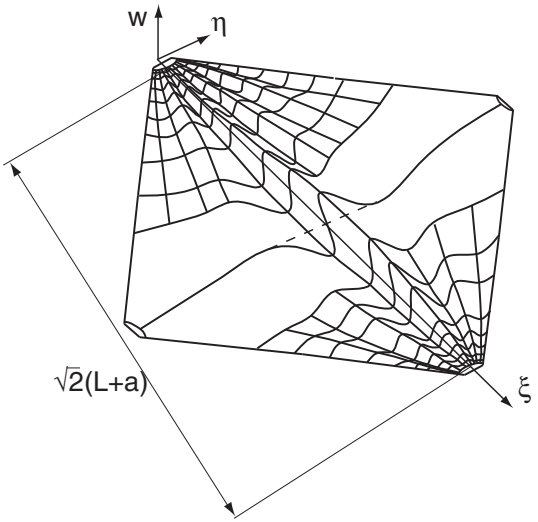

Figure 13. Wrinkle pattern for $T_1/T_2 \geq 1/(\sqrt{2}-1)$.

where λ is the half-wavelength, and A the maximum amplitude. We will follow the same procedure of Section 5.2 to estimate the wavelength of this wrinkle.

The longitudinal and transverse curvatures, obtained by differentiating Equation (66), are

$$\kappa_\xi = -\frac{\partial^2 w}{\partial \xi^2} = \frac{A\pi^2}{2(L+a)^2} \sin\frac{\pi\xi}{\sqrt{2}(L+a)} \sin\frac{\pi\eta}{\lambda},$$

$$\kappa_\eta = -\frac{\partial^2 w}{\partial \eta^2} = \frac{A\pi^2}{\lambda^2} \sin\frac{\pi\xi}{\sqrt{2}(L+a)} \sin\frac{\pi\eta}{\lambda},$$

and the corresponding maximum values, at the centre of the membrane, are

$$\tilde{\kappa}_\xi = \frac{A\pi^2}{2(L+a)^2}, \qquad \tilde{\kappa}_\eta = \frac{A\pi^2}{\lambda^2}. \tag{67}$$

The longitudinal stress at the centre of the wrinkle is obtained by determining the wedge angle θ_1, as explained in Section 5.1, and then noting that at the centre of the membrane ξ and r are parallel. Hence,

$$\sigma_\xi = \frac{T_1}{\sqrt{2}(L+2a)t\sin\theta_1}. \tag{68}$$

The transverse stress, σ_η, at the centre of the wrinkle is given by Equation (4), as usual. Substituting Equations (67), (68) and (4) into Equation (5), and then solving

for λ gives

$$\lambda = \sqrt[4]{\frac{\pi^2 E t^3 (L+2a)(L+a)^2 \sin\theta_1}{3\sqrt{2}(1-\nu^2)T_1}}. \tag{69}$$

The calculation of the wrinkle amplitude is different from the earlier case, as now we are dealing with a localised wrinkle. Hence, instead of working in terms of strains, we will consider the total extensions along the diagonals of the membrane.

We begin by noting that the variable angle wedge stress field involves slack regions along all four edges of the membrane. Hence, neglecting the effects of any out-of-plane deformation, we can think of the edges of the membrane simply as four rigid links connected by pin-joints, and hence forming a square four-bar linkage. Therefore, since the corners of the membrane subjected to the loads T_1 move outwards, each by δ_1 (whose value can be estimated with (53), for $i = 1$), the corners subjected to the loads T_2 move *inwards* by δ_1. Therefore, the extension of the diagonal parallel to the loads T_2 is $-2\delta_1$.

This extension includes a component due to elastic stretching, found by integrating the elastic strains along the diagonal, and hence given by $2\delta_2$. The value of δ_2 can be estimated with Equation (53), for $i = 2$. It also includes a component due to the geometric strain induced by the single wrinkle, which can be found by multiplying the wave-length, 2λ, by the wrinkling strain, Equation (18); this gives $-\pi^2 A^2/2\lambda$. Therefore, we obtain

$$-2\delta_1 = 2\delta_2 - \frac{A^2\pi^2}{2\lambda}$$

and, solving for A,

$$A = \frac{2\sqrt{\lambda(\delta_1+\delta_2)}}{\pi} \tag{70}$$

where λ is given by (69) and δ_1, δ_2 are given by (53).

6. Validation of analytical results

The analytical predictions of the wrinkle details, developed in Sections 4 and 5.2 will now be compared against a variety of "reference" results obtained experimentally or numerically, on Kapton HN® membranes with measured Young's modulus $E = 3500$ N/mm^2 and Poisson ratio $\nu = 0.31$ [Wong and Pellegrino 2005a].

6.1. ***Membrane in shear.*** The dimensions of the membranes were $H = 128$ mm by $L = 380$ mm.

To begin with, we consider the average magnitude of the midsurface minor principal stress, i.e., the compressive stress across the wrinkles, acting at midheight. This stress would be difficult to measure experimentally, but can be readily obtained

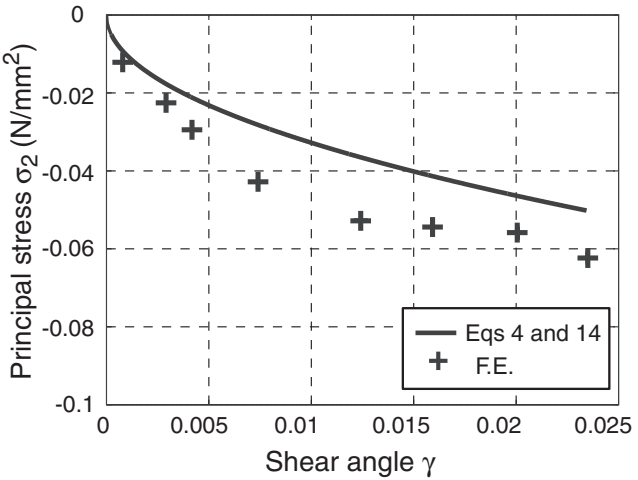

Figure 14. Minor principal stress at midheight, for 0.025 mm thick Kapton membrane in shear.

from a detailed finite-element simulation where the membrane is represented by thin-shell elements.

Figure 14 compares, for different values of the shear angle, the average stress obtained in [Wong and Pellegrino 2005b] with analytical predictions obtained by substituting (14) into (4). The largest discrepancy between the analytical predictions, which do not take into account the fans of wrinkles at either end of the membrane, and a very detailed finite element simulation is never more than 30%.

Next, we consider the relationships between the wrinkle wavelength, 2λ, and the amplitude, A, with the angle of shear, γ, provided by (14) and (22), respectively. Figures 15 and 16 show plots of these relationships, together with a large set of experimental results obtained from Kapton membranes of three different thicknesses, and a set of finite-element simulation results, obtained in [Wong and Pellegrino 2005b]. Both sets of results bunch closely along the analytical predictions.

6.2. ***Membrane under corner loads.*** The geometrical parameters of the membrane were $L = 472$ mm, $a = 17$ mm, and $t = 0.025$ mm.

First, we consider the membrane loaded by four equal forces. For this case we will focus on the corner load-displacement relationship and the details of the corner wrinkles.

Figure 17 compares the predictions of the corner displacements from Equations (37) and (39) (both of which are known to provide upper-bound estimates on the correct displacement) with two sets of reference values, obtained from two different types of finite element models [Wong and Pellegrino 2005b].

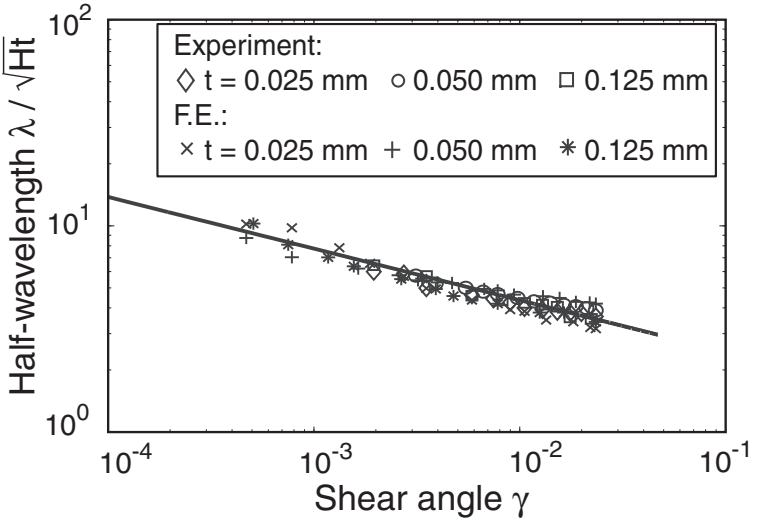

Figure 15. Comparison between nondimensional wrinkle half-wavelength from Equation (14) (solid line) and two sets of reference results, for membrane in shear.

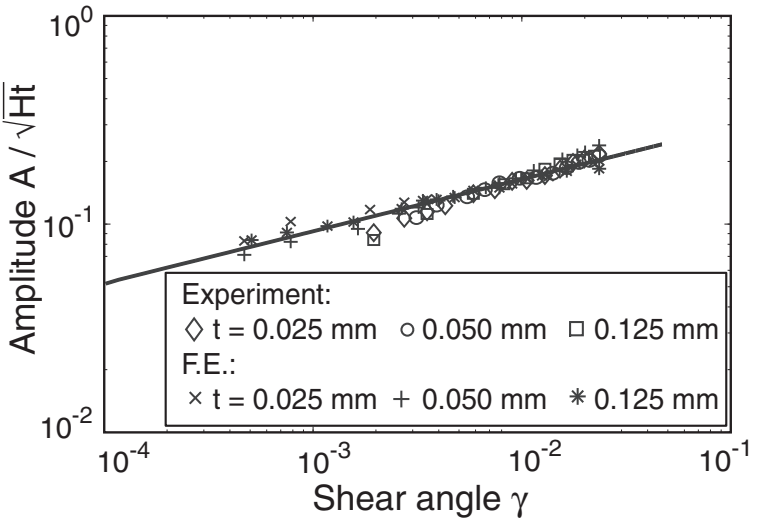

Figure 16. Comparison between nondimensional wrinkle amplitude from Figure 16 (solid line) with two sets of reference results, for membrane in shear.

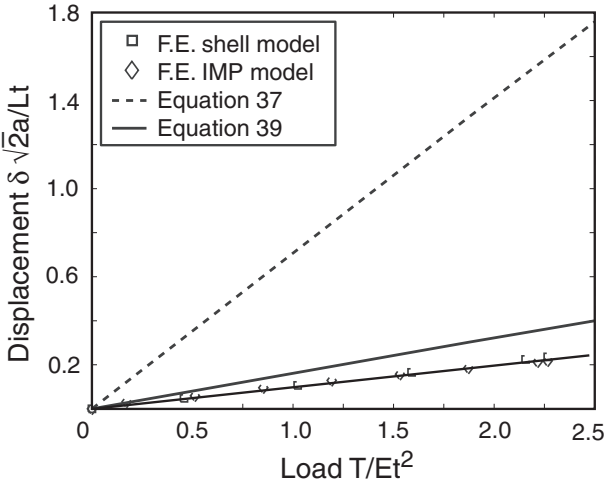

Figure 17. Relationship between nondimensional corner displacement and load, for symmetric loading of square membrane.

The two sets of finite-element results fit almost exactly on a straight line, and both analytical predictions are also linear. Equation (39), based on the wedge field, gives much closer predictions than (37), based on the diagonal strip field. This suggests that, among these two, the wedge field provides a much more accurate approximation to the actual stress distribution in the membrane when equal corner loads are applied.

Table 1 compares the number of corner wrinkles and their maximum amplitude, predicted using Equations (60) and (63), with direct experimental measurements [Wong and Pellegrino 2005a] and results from finite-element simulations using a thin-shell model [Wong and Pellegrino 2005b], for two different load levels, $T = 5$ N and 20 N.

	n			A (mm)		
	Equation (60)	Exp.	F.E.	Equation (63)	Exp.	F.E.
$T = 5$ N	11.3	8	8	0.14	0.12	0.12
$T = 20$ N	16.0	11	9	0.20	0.14	0.16

Table 1. Number of corner wrinkles, n, and their maximum amplitude, A, under symmetric loading.

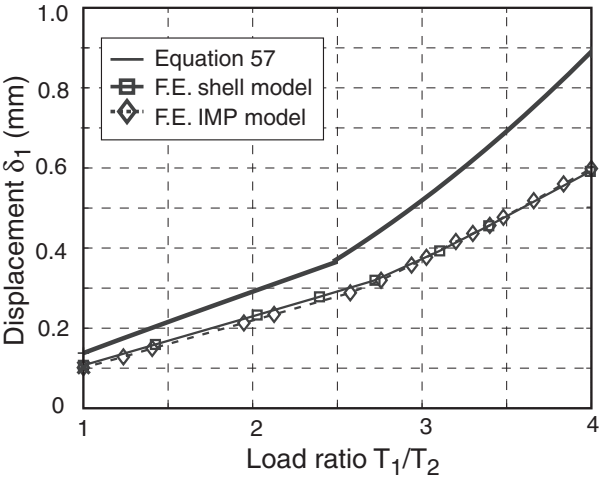

Figure 18. Relationship between corner displacement and load ratio, for asymmetric loading of square membrane.

The number of wrinkles predicted by Equation (60) is typically a 40% overestimate of the number observed in the experiments, whereas the simulation results match the experiments much more closely. It is not surprising that the analytically predicted number of wrinkles should be in excess of the actual number, since we have assumed a uniform fan of wrinkles whereas in reality there are no wrinkles along the edges Wong and Pellegrino [2005a, Figure 9].

The predicted wrinkle amplitudes are also overestimates, by 15% to 40%, due to the fact that in a real membrane a significant amount of out-of-plane displacement associated with wrinkling takes place along the edges of the region.

Next, we consider the same membrane and, while keeping two of the corner forces constant at $T_2 = 5$ N, we increase the other two forces, T_1, until the ratio between T_1 and T_2 becomes 4. For this case we will focus on the relationship between corner displacement and load ratio, and on the diagonal wrinkle.

Figure 18 shows a plot of Equation (53) for the diagonal displacement of the most heavily loaded corners vs. the ratio T_1/T_2, plus two sets of reference results, obtained from two different finite-element models [Wong and Pellegrino 2005b] which have given substantially identical results. An alternative, and simpler, prediction, could be obtained from Equation (30), however we have already seen for the case of symmetric loading that the predictions from this equation are poor.

The main observation from Figure 18 is that the reference response shows an approximately bilinear variation of δ_1, with softening by about 30% at $T_1/T_2 \approx 2.7$. This decrease in stiffness coincides with the formation of a large diagonal

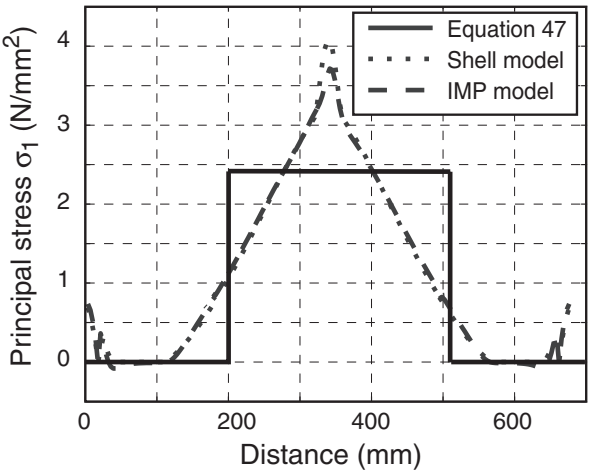

Figure 19. Distribution of midsurface principal stress along a diagonal, for $T_1/T_2 = 4$.

wrinkle. The response predicted by Equation (53) follows the same general trends as the reference solution, but the value of T_1/T_2 at which the slope changes is underestimated by about 10% and the predicted slopes are over-estimated by about 10% and 60%, respectively before and after the slope transition.

Incidentally, the initial mismatch between the two solutions, at $T_1/T_2 = 1$, is largely due to fact that the finite-element models include the corner tabs that were used in our experiments [Wong and Pellegrino 2005a].

It is interesting to compare the distribution of the midsurface, major principal stress along a diagonal, shown in Figure 19. The variation of σ_1 derived from the variable-angle wedge field is a square wave, whereas the finite-element simulations show an almost triangular wave. The stress increases near the corners; also note that the assumed stress field underestimates the peak stress by about 60%.

Finally, Table 2 compares our analytical predictions of the diagonal wrinkle details when $T_1/T_2 = 4$, for two different membrane thicknesses, $t = 0.025$ mm and $t = 0.050$ mm. Experimental results from [Wong and Pellegrino 2005a] and finite-element simulation results from [Wong and Pellegrino 2005b] are provided for comparison.

Regarding the half-wavelength presented in Table 2, our predictions for the thinner membrane practically coincide with the experimental measurements and the FE simulations. For the thicker membrane, Equation (69) over-estimates λ by about 15%.

Regarding the wrinkle amplitude, it can be predicted in two different ways. The most direct method is to follow a fully analytically approach, and hence to

	λ (mm)			A (mm)			
t (mm)	Eq. (69)	Exp.	F.E.[a]	Eq. (70)+(53)	Eq. (70)+F.E.[b]	Exp.	F.E.[b]
0.025	24.6	25.4	22.3	3.55	2.8	1.89	2.02
0.050	41.3	33.9	35.6	3.25	2.1	1.81	1.63

Table 2. Half-wavelength, λ, and amplitude, A, of diagonal wrinkle for $T_1/T_2 = 4$. [a] shell model. [b] IMP model.

estimate δ_1 and δ_2 from Equation (53), and substitute their values into Equation (70). Alternatively, one can estimate δ_1 and δ_2 with a finite-element stress analysis that uses no-compression elements, such as the IMP model used in [Wong and Pellegrino 2005b]. The corresponding results are presented in columns 5 and 6 of Table 2.

The fully analytical estimates are up to 88% higher than the experimental measurements. However, the error decreases, to 48% and 16%, respectively for the thinner and thicker membranes, when Equation (70) is combined with the finite-element estimates.

7. Discussion and conclusions

This paper has presented a general analytical framework for thinking about the location and pattern of wrinkles in thin membranes, and for making preliminary estimates of their wavelength and amplitude.

The key ideas in the analytical model that has been proposed are as follows. First, the wrinkled region and the direction of the wrinkles can be determined from a two-dimensional stress field that admits no compressive stress anywhere, satisfies equilibrium, and provides a reasonably close (upper) bound to the actual complementary strain energy of the membrane. Second, the wavelength of the wrinkles can be estimated by considering a (small) compressive buckling stress in the direction transverse to the wrinkles, and by ensuring that this stress component and the longitudinal stress (given by the two-dimensional stress field) are in equilibrium in the out-of-plane direction, say, at the centre of the wrinkles. Third, the amplitude of the wrinkles is determined by matching the sum of the material strain and geometric strain due to wrinkling, in the direction transverse to the wrinkles, to the boundary conditions imposed by the nonwrinkled region.

This analytical model has been applied to two different problems, a rectangular membrane under simple shear and a square membrane loaded at the corners.

In the first problem, the wrinkles are essentially uniform and the stress field is known. Our model predicts the wavelength and the wrinkle amplitude to be

respectively *inversely proportional* and *directly proportional* to the fourth root of the shear angle; see Equations (14) and (22). Both values are *directly proportional* to the square root of the height and thickness of the membrane, and both are independent of the Young's modulus.

In the second problem two wrinkling regimes have been identified. The first is characterised by relatively uniform, small, radial corner wrinkles and occurs for load ratios smaller than $1/(\sqrt{2}-1)$. The number of radial wrinkles is proportional to the fourth root of the radius of the wrinkled region and the corner forces; see Equation (60). The amplitude of these wrinkles is inversely proportional to this number and directly proportional to the square root of the radius of the wrinkled region and to the corner force; see Equation (63). Here the radius of the wrinkled region is proportional to the radius of the uniaxially stressed wedge field (Equation (65)).

The second regime occurs for load ratios larger than $1/(\sqrt{2}-1)$, and is characterised by a large diagonal wrinkle, plus small radial wrinkles at all four corners. The variation of the width and amplitude of this wrinkle are more complex — see Equations (69) and (70) — since the geometric parameters of the stress field are dependent on the load ratio, through Equations (47), (50), and (52).

Acknowledgements

The authors thank Professor C. R. Calladine, FRS, Dr. K. Belvin and Professor K. C. Park for useful discussions and suggestions. Helpful suggestions by an anonymous reviewer are gratefully acknowledged. Financial support from NASA Langley Research Center (research grant NAG-1-02009, technical monitor Dr. K. Belvin) and the Cambridge Commonwealth Trust is gratefully acknowledged.

References

[Calladine 1983] Calladine, C. R., 1983. Theory of Shell Structures. Cambridge University Press, Cambridge.

[Cerda and Mahadevan 2003] Cerda, E., and Mahadevan, L., 2003. Geometry and physics of wrinkling. Physical Review Letters, **90**, no. 7.

[Epstein 2003] Epstein, M., 2003. Differential equation for the amplitude of wrinkles. AIAA Journal, **41**, 327–329.

[Epstein and Forcinito 2001] Epstein, M., and Forcinito, M. A., 2001. Anisotropic membrane wrinkling: theory and analysis. International Journal of Solids and Structures, **38**, 5253–5272.

[Haseganu and Steigmann 1994] Haseganu, E. M. and Steigmann, D. J. 1994. Analysis of partly wrinkled membranes by the method of dynamic relaxation. Computational Mechanics, **14** 596–614.

[Jenkins and Leonard 1991] Jenkins, C. and Leonard, J. W., 1991. Nonlinear dynamic response of membranes: State of the art. ASME Applied Mech. Reviews, **44**, 319–328.

[Ligaro and Valvo 2000] Ligaro, S., and Valvo, P. S., 2000. Stress distribution around discontinuities in soft elastic membranes. IASS-IACM 2000 Computational Methods for Shell and Spatial Structures (Edited by Papadrakakis, M., Samartin, A., and Onate, E.), Chania, Crete.

[Lin and Mote 1996] Lin, C. C., and Mote, C. D., 1996. The wrinkling of rectangular webs under nonlinearly distributed edge loading. Journal of Applied Mechanics, **63**, 655–659.

[Mansfield 1968] Mansfield, E. H., 1968. Tension field theory a new approach which shows its duality with inextensional theory. Proc. 12th Int. Congress Applied Mechanics, 305–320.

[Mansfield 1970] Mansfield, E. H., 1970. Load transfer via a wrinkled membrane. Proceedings of the Royal Society of London Part A, **316**, 269–289.

[Mansfield 1981] Mansfield, E. H., 1981. Gravity-induced wrinkle lines in vertical membranes. Proceedings of the Royal Society of London Part A, **375**, 307–325.

[Mansfield 1989] Mansfield, E. H., 1989. The bending and stretching of plates, second edition. Cambridge University Press, Cambridge.

[Murphey et al. 2002] Murphey, T., Murphy, D., Mikulas, M. M., and Adler, A. L., 2002. A method to quantify the thrust degradation effects of structural wrinkles in solar sails. 43rd AIAA/ASME/ASCE/AHS Structures, Structural Dynamics, and Materials Conference, Denver, Colorado, AIAA-2002-1560.

[Pipkin 1986] Pipkin, A. C., 1986. The relaxed energy density for isotropic elastic membranes. IMA Journal Applied Mathematics, **36**, 85–99.

[Reissner 1938] Reissner, E., 1938. On tension field theory. Proceedings 5th International Congress of Applied Mechanics, 88–92.

[Rimrott and Cvercko 1986] Rimrott, F. P.J., Cvercko, M., 1986. Wrinkling in thin plates due to in-plane body forces. In: Inelastic behaviour of plates and shells, (Edited by L. Bevilacqua, R. Feijoo and R. Valid), 19–48. Springer-Verlag.

[Roddeman et al. 1987] Roddeman, D. G., Drukker, J., Oomens, C. W.J., Janssen, J. D., 1987. The wrinkling of thin membranes: Part I–Theory. Journal of Applied Mechanics, **54**, 884–887.

[Steigmann 1990] Steigmann, D. J., 1990. Tension Field Theory. Proceedings of the Royal Society of London Part A, **429**, 141–173.

[Stein and Hedgepeth 1961] Stein, M., Hedgepeth, J. M., 1961. Analysis of partly wrinkled membranes. NASA Langley Research Center, NASA TN D-813.

[Timoshenko and Goodier 1970] Timoshenko, S. P., and Goodier, J. N., 1970. Theory of Elasticity. Third edition ed., McGraw-Hill, Tokyo.

[Wagner 1929] Wagner, H., 1929 Flat sheet metal girder with very thin metal web, Zeitschrift f*ü*r Flugtechnik Motorluftschiffahrt. **20**, 200–207, 227–233, 256–262, 279–284.

[Wong and Pellegrino 2002] Wong, Y. W. and Pellegrino, S., 2002. Amplitude of wrinkles in thin membrane. New Approaches to Structural Mechanics, Shells and Biological Structures, (Edited by H. Drew and S. Pellegrino), Kluwer Academic Publishers, 257–270.

[Wong et al. 2003] Wong, Y. W., Pellegrino, S., and Park, K. C. 2003. Prediction of wrinkle amplitudes in square solar sails. In Proc. 44th AIAA/ASME/ASCE/AHS/ASC Structures, Structural Dynamics, and Materials Conference and Exhibit, AIAA-2003-1980.

[Wong and Pellegrino 2005a] Wong, Y. W. and Pellegrino, S. 2006a. Wrinkled membranes I: experiments. Submitted for publication.

[Wong and Pellegrino 2005a] Wong, Y. W. and Pellegrino, S. 2006a. Wrinkled membranes I: experiments. J. of Mechanics of Materials and Structures **1**, 2–23.

[Wong and Pellegrino 2005b] Wong, Y. W. and Pellegrino, S. 2006. Wrinkled membranes III: numerical simulations. J. of Mechanics of Materials and Structures **1**, 61–93.

[Wu 1978] Wu, C. H. 1978. Nonlinear wrinkling of nonlinear membranes of revolution. Journal of Applied Mechanics, **45**, September, 533–538.

[Wu and Canfield 1981] Wu, C. H. and Canfield, T. R. 1981. Wrinkling in finite plane-stress theory. Quarterly Journal of Mechanics and Applied Mathematics, **39**, 2, 179–199.

Received 3 Mar 05. Revised 10 Oct 05.

Y. WESLEY WONG: wesleywong@cantab.net

SERGIO PELLEGRINO: pellegrino@eng.cam.ac.uk
Department of Engineering, University of Cambridge, Trumpington Street, Cambridge, CB2 1PZ, United Kingdom